A. Rivolta, P. Lunghi, M. Lavagna
GNC & Robotics for on Orbit Servicing with Simulated Vision in the Loop
Acta Astronautica, Vol. 162, 2019, p. 327-335
doi:10.1016/j.actaastro.2019.06.005

GNC & Robotics for on orbit servicing with simulated vision in the loop

Aureliano Rivolta[a,*], Paolo Lunghi[a], Michèle Lavagna[a]

[a] *Politecnico di Milano, Via La Masa, 34 20156 Milano - Italy*

Abstract

Complex robotics missions require complex GNC and Robotics algorithms, often using vision sensors. The problem of vision-in-the-loop GNC is addressed using photorealistic simulated images and simple computer vision algorithms, coupled with relative estimation and control of a servicing satellite in close proximity operations with a customer satellite. In the near future it will be required to simulate the behavior of automated servicing missions comprehending also vision data, hence the request for vision-in-the-loop simulations. In this article is proposed a GNC and Robotics scheme for proximity operations between a servicer and a customer satellite through the use of adaptive control and computer vision. The scheme is then put to test through simulation of orbital robot dynamics, sensors and camera inputs, and computer vision algorithm in the loop.

Keywords: On Orbit Servicing, Guidance, Navigation, Control, Robotics, Computer Vision, Image simulation

1. Introduction

On Orbit Servicing (OOS) is a hot topic in the space community and source of continuous research. Recently contracts have been signed by interested parties

*Corresponding author
Email address: aureliano.rivolta@polimi.it (Aureliano Rivolta)

and some providers[1][2], others (Airbus for example[3]) are starting to display the intent to bring OOS to life in the next couple of years.

Although the customer demand is unclear, the added value OOS can give to operators is higher flexibility [1, 2]. This changes perspective in the analysis of the business case [3, 4, 5] that must also take into account the current level of OOS technology [6].

Since the first OOS was achieved by astronaut's Extra Vehicular Activity (EVA) on Intelsat VI and the Hubble space telescope during the STS-49 and STS-61 missions there has been widespread research on how to expand the concept without EVAs.

In the years the concept of automated resupply to the International Space Station (ISS) has been perfected, especially by the European Automated Transfer Vehicle (ATV) program [7], the Japanese H-II Transfer Vehicle (HTV) [8], and in recent years, by private owned resupply spacecraft like Dragon [9] and Cygnus [10]. However, the ISS is one of a kind and commercial OOS involving civilian and non civilian endeavors requires a different perspective. Space industry is bound to be mostly driven by military and private companies and economic exploitation of OOS is the main concern for the latter, hence any OOS mission shall be sustainable in a market perspective without relying continuously on governmental agencies founds.

The most lucrative area for OOS is Geostationary Earth Orbit (GEO) where major telecommunications operator assets are located. However, in Medium Earth Orbit (MEO) we have positioning systems like GPS or Galileo that could benefit from OOS. If we include in OOS also debris removal, then it will be Low Earth Orbit (LEO) to be exploited first. Moving asset from orbit to orbit is also an interesting concept that exemplifies further that OOS is actually not bounded in some particular orbital region.

[1] http://spacenews.com/effective-space-signs-first-contract-for-satellite-life-extension-services/

[2] http://spacenews.com/orbital-atk-lands-second-intelsat-satellite-servicing-deal/

[3] http://spacenews.com/airbus-to-challenge-ssl-orbital-atk-with-new-space-tug-business/

	Physical	Retro-compatibile	Customer mods	References
Refueling	yes	no	small	[22]
Payload upgrade	yes	no	huge	[23]
Orbit insertion / Tugging	yes	yes	none	[24, 25]
Repair	yes	no	huge	[23]
Inspection	no	yes	none	[24]

Table 1: OOS concepts

There are many technological challenges on the road to achieve robotic/automated OOS, which have sparked various research programs in the last decades. For example the Defense Advanced Research Projects Agency (DARPA) funded Orbital Express mission successfully demonstrated autonomous rendezvous and docking [11, 12, 13] and refueling operations [14]. During the mission also berthing and servicing functionality have been accomplished [15]. Robotic manipulators can be used to grab, un-dock and replace units and this capability has been also demonstrated by the Engineering Test Satellite VII (ETS-VII) of National Space Development Agency (NASDA) where autonomous rendezvous and berthing, visual servoing, units exchange and refueling have been accomplished [16, 17, 18, 19]. One of the robotic arm experiments onboard ETS-VII was prepared by the Deutsches Zentrum für Luft- und Raumfahrt (DLR) and was part of the agency research plans for OOS [20]. Such feats were accomplished also thanks to previous missions like the STS-72 with the retrieval of the Space Flyer Unit [18].

In this section the presentation of many OOS scenarios is carried out to establish the base of the subsequent technical analysis. The list is meant to be introductory not comprehensive as combination of scenarios permits to obtain new servicing possibilities; it can be found in Table 1. The table classifies main OOS scenarios based on the need of physical connection, on the possibility to propose the service to already flying satellites and the eventual customer satellite modification needed for acquiring compatibility; some references are also included. For more depth in each of these possible scenario, please refer to [21].

Looking at the scenarios presented before, the main capabilities required for

a servicing satellites are: rendezvous, formation flying with customer, repeated docking, target pointing, superior attitude control authority, intersatellite communication, robotic manipulation and a fuel feeding system. Although some proposed a vehicle with all such capabilities [26], it is more likely to see specialized servicing vehicles in the near future with limited and selected capabilities.

All of the above require a dedicated Guidance Navigation & Control (GNC) subsystem as well as handling robotics arm and similar hardware. This will be the core of this article with particular focus on the use of image based sensors. In order to assess the performance and goodness of the architecture that will be presented it is clear that simulations, at least numerical, are required[4]. Among the lesson learned from the Orbital Express mission we could list a requirement for extensive sensor and navigation testing prior to mission execution [27]. One of the main issues is the need to simulate image based data with enough representativity to understand the level of precision that can be reached.

The focus of the work is the use of vision based estimation within a GNC loop, hence an overview of both part is required to understand how they can work together. The article is thus divided into four sections. Section 2 presents computer vision applications while Section 3 specializes in the developed applications of vision based sensing in the OOS framework; Section 4 presents the algorithms used for the GNC and robotics, where it has been used the term Guidance Navigation Control & Robotics (GNCR) to put under the same bracket the vehicle GNC and the robotic equivalent GNC. The proposed control architecture with simulated images is then tested in Section 5 using custom

[4]An example is the company Effective Space Solutions testing at GMV: "GMV is in charge of supporting the development of the service mission with several activities related to the execution of hardware-in-the-loop test campaigns in GMV's platform-art© facility. [...] At the moment GMV is busy developing one of the critical components of the SPACE DRONE^{TM} RvD system, i.e., the image processing algorithm that will be used for detecting the customer's GEO host satellite and computing its position and attitude during the rendezvous maneuver" extract from press release available at https://www.gmv.com/en/Company/Communication/News/2018/03/EffectiveSpace.html

made code running on MATLAB®, Simulink® and POV Ray.

2. The use of images in OOS

Computer vision algorithm for navigation can assume in general two different forms: image stream and template/map/model matching. Image stream techniques compute the relative movement between two consecutive images by comparing displacement of pixels or notable features of the scenery. Instead, template matching compares a single image with a database or model of known features. This require prior knowledge on the scenery and a proper configured source to use for the comparison. All these algorithms usually require other sensors or models to provide a stable and precise estimation.

Template matching for proximity operations using cameras has been studied in the past and implemented in orbit in relation to cooperative docking. In [28] are shown several markers used for cooperative rendezvous and docking. An example is the ETS-VII mission where markers and vision tracking have been used in several experiments [29, 30]. Markers and reflectors allow increased performance in the relative state estimation but requires the customer satellite to be built accordingly. Template matching can be used even in case where such features are not installed but are extracted from the geometry of the customer satellite. [31] has implemented a 3D matching using non linear minimizers to solve the pose, although images were not simulated and the computer vision part has been neglected. A more recent and comprehensive reference with experimental validation can be found in [32] where 3D model matching is combined with a visual servoing approach. Further development on exploiting the maximum return from images can be found in [33] while the basis for 3D matching have been posed more than two decades ago, the interested reader should refer to [34].

Image stream techniques can be roughly divided in feature tracking and optical flow. The great limitation of the latter is the weakness to large displacement, hence a minimum sampling time would be requested based on the

relative dynamics of the target. On the other hand, feature tracking requires to detect features of the same kind in two images and then apply a matching procedure, a rather costly operation. Features can be divided roughly in low level (edges, corners) and high level (ex: landmarks). High level feature are usually combinations of low level features, hence more expensive to track. In the last decade the new concept of region based feature has been studied. *Scale Invariant Feature Transform* (SIFT in short) [35], *Speeded Up Robust Features* (SURF) [36, 37] and ORB [38] lie within this category: the basic principle it to take interesting low level points such as corners and identifying those with better probability to be traced in the other image.

Some research groups have been working on the use of vision based relative state estimation based on known features on the target satellite, for example in [39, 40] matching is done with a rectangular shape, while in [41] the adapter ring is exploited. A more sophisticated and robust implementation of similar principles is found in [42].

3. Application to relevant OOS scenarios

OOS proximity operations, including inspection, may require the use of vision-based navigation. For far-range inspection the pointing required is not too harsh, but reliability in the navigation system is extremely important [27]. Close proximity operations require similar level of reliability, but the precision requested is higher. While at large distances the only information needed about the target is the relative position, at close distance also the attitude become relevant, and the required image processing differs from far approach operations. Sensor complementary to cameras might differ depending on application. In the far range relative GPS might be an extremely valuable source of information, while when the two spacecrafts are close laser based applications might have a better impact. Image based navigation is not perfect and has limitations but can be used to extract useful information to estimate the relative state of the customer satellite or other meaningful information. A proposed application for

relative state estimation and port location refinement follows in this section.

3.1. Hardware limitations

The application of image processing techniques on space hardware are usually limited by the high required computational burden. In recent years, an effort has been made by space industry to qualify dedicated hardware capable to provide the necessary processing power. In [43], an image processing board, capable to perform feature extraction and tracking task at 20 fps on a 1024×1024 pixels image, is presented. A similar, space qualified, processing unit is described in [44] and [45], with the capability to perform both monocular and stereo visual navigation in a framerate range from 10 to 30 fps. In this paper, a conservative value of 1 fps is assumed, to ensure compatibility of the developed algorithms with the future available space hardware.

3.2. Satellite relative state

A single camera can be used to estimate the relative state of the servicer satellite when it is within meters from the customer satellite. Here is presented a simplified approach used as demonstration for closed loop performance estimation. Such algorithm would need to be improved for robustness of the estimation in future development. The process of information extraction from a single image is divided in four steps:

- Edge detection,
- Constrained line search,
- Depth estimation,
- Relative pose estimation.

First, the image is processed with a Sobel edge detector to produce a binary image where lines are easily found with the Hough transform. Then, four lines are extracted, two vertical and two horizontal, within a 5 degree inclination domain.

This limitation on the search domain increases the robustness in the line-fitting process but can be adopted only during terminal phases when a partial alignment between the servicer and the target is already attained. In space, largely variable light conditions can affect the edge detection process. In [42] the issue is addressed by looking for the tracked lines in a subspace of the whole search space.

The simplified idea of tracking a relatively known rectangular shape has also been applied experimentally with compatible results in [46]. The four tracked lines are used to compute the four corner points in the image.

A precise estimation of the scene depth is performed by minimization of the projection error. Displacement and attitude are computed using a combination of the dual quaternion estimation of [47] and [48].

The limits imposed in the line search need to be tailored as many sources of error can affect the final estimation. These might include shadows projected by robotic arm, specific illumination directions that can make other lines sharper than the outer edges, or light reflections on metallic surfaces that might reduce the local image gradient, exploited by most of the algorithms for line detection. In general, fast light variations can have dramatic impact on the cameras, although these can be somehow predicted. There are some cases where the light positioning is not favorable, for example when the sun is behind the servicer satellite: the spacecraft casts shadows altering the image histogram and creating troubles in the segmentation process. Simulated images can be used to infer possible criticalities of operations and prepare solutions or scheduling accordingly.

3.3. Robotic arm and docking port

When a robotic arm is involved in close proximity operations for grabbing or operating on the customer satellite, making use of cameras mounted on the tip can give a lot of insights and feedback to the robotic subsystem. However, due to the tip being close to the target we have that the images recorded are subject to blurring or self-shadowing. Both phenomena can be caused by distances below

one meter, after that the robustness of the system might be compromised. One possible way to solve the problem is to use lights and auto-focus cameras at higher hardware expenses. What we propose instead is to use a simple camera mounted on the tip to refine the position of the target (a docking port in this case) with respect to the reference used for relative positioning mentioned in the previous section. Through chain of transformation the measures can be used to estimate the port location on the target satellite and control the robotic arm accordingly.

In the subsequent simulations markers have been used: four circles of two different colors (white and black) on an intermediate background. Using Hough transform and a initial distance estimation the algorithm will find circles in a neighborhood of the estimated circle diameter. Once all four circle position are computed in camera frame, the relative attitude is computed using four directions of the markers with respect to their center and the normal of the plane identified by the 3D positions of the markers in the model reference of the target satellite. The 3D position of the markers is recovered by using the radius of the circle found in the images as scale factor, thus the estimation becomes really fast.

Like in the previous case it is mandatory to apply bounding of parameters, otherwise serious discrepancies in subsequent estimation can be found. The final estimation is performed by a weighted mean where weights are computed as the overall fitting error. The finalization of the port location requires the port to be visible, hence the expected error is small and any simplification made is justified.

3.4. Simulation of images in the loop

When dealing with closed loop GNC aided by vision sensor, it is mandatory to have a good model to represent the camera but this is rarely done due to computational burden. For example in [31] images were not used in the loop but rather points and lines were assumed almost-perfect. In cases where images are generated, they might lack some realistic aspects, like images in [41] that were

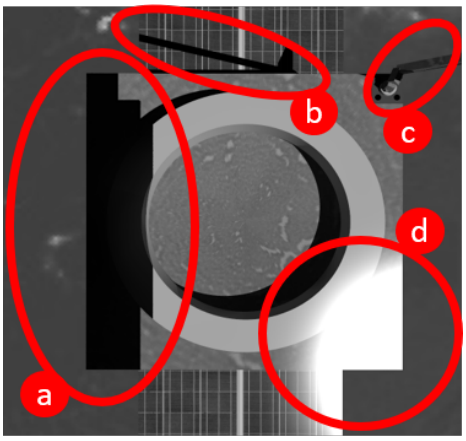

Figure 1: Details of POV Ray based image rendering: a) servicer satellite shadow b) robotic arm shadow c) robotic arm d) sunlight reflection

not rendered with Earth in sight, self-shadows and shadows induced by servicer nor reflections: the quality of images is by far greater than in the real scenario. This is true most of the time as also noise introduction is quite cumbersome to add. Increasing image sensor accuracy means to make use of advanced rendering techniques that require a lot of computation to be created, increasing notably by 5 or 10 times the total simulation time of the feedback loop.

In this work the images are rendered using POV Ray[5], a software based on ray-tracing. This technique is the best technique to obtain photorealistic images as it reproduces the physical processes of light propagation. The photorealistic performance of POV Ray are testified in [49] where the commercial software PANGU, approved by ESA, has been validated using POV Ray itself. POV Ray has also been used with success to generate images for artificial intelligence applied to lunar landing hazard detection in [50] and subsequent works.

The important features that a POV Ray generated image can make are realistic reflections and shadows cast by several objects. By adding an Earth

[5]Persistence of Vision Pty. Ltd. (2004) Persistence of Vision Raytracer (Version 3.6) [Computer software]. Retrieved from http://www.povray.org/download/

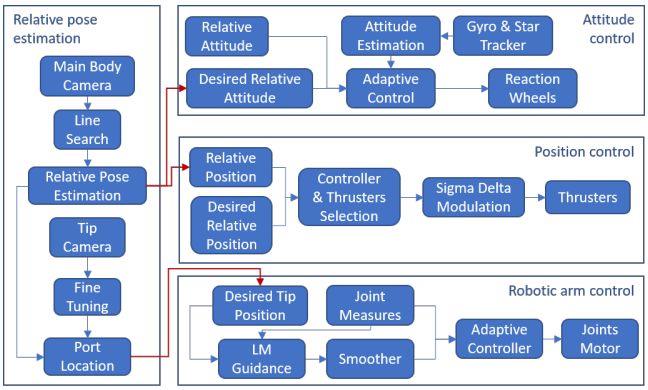

Figure 2: Guidance Navigation Control and Robotics scheme

textured sphere one can include the disturbance for computer vision software of a background. Should be noted that the texture here used is by far not high-definition, hence closeups might look poor. Enhancing the textures would require more processing power, hence the compromise. All these features can be seen directly in Figure 1, where shadows induced by the servicer satellite and its robotic arm, as well as reflection induced by the sunlight on metallic components are highlighted in red.

Difficult aspects to include in POV Ray images are the sun in sight and the image noise. Noise is added as a positive bias and random integer addition for each pixel. This allows to create noise that can reduce gradient based feature extraction performance of an otherwise polished image and shift the histogram of the image as perfect blackness is rarely found in navigation cameras.

4. The GNCR loop

Figure 2 gives an overview of the GNCR loop here proposed for proximity operations. The system can be divided in three control loops, one for the attitude control, one for the relative positioning control and one for the robotic arm. The estimation of the relative state and location of docking port or key features plays the role of feeding information to all the other control loops. Every action taken by each of the control segment influences the camera output that, after

being processed, return new reference for the loop themselves. All the GNCR elements are thus interconnected. The relative position control loop aims to control the center of mass of the orbital robot with respect to the customer satellite exterior, thus uses the camera relative distance estimation to maintain a relative position. Drifts due to orbital dynamics and robotic arm motion have to be counteracted. The attitude control problem is subject to more disturbances as the inertia of the system varies due to robotic arm motion and is a very critical system for all the space segment mission. Attitude estimation and adaptive control are thus explored here. Finally, the robotic arm control uses the compute position and attitude of the target feature (here a small docking port) to determine the required joint position and generates a smooth trajectory for the joints to follow. Trajectory generation is the focus of the development, while the control is an extension of the adaptive controller used for the attitude problem.

4.1. Position & thrusters control

Position control for proximity operations use the relative state estimation to determine the force that needs to be used by the servicer to reach and maintain a certain pose with respect to the target. Such control forces are computed using a classical approach. Relative position measured by cameras is rotated on a Local Vertical Local Horizontal frame whose simplified dynamics can be used to derive a PD-like approach.

The only mean to control a satellite position for precision operations is to use thrusters. Those thrusters are positioned usually near the corners and sides of a satellite so that they are also able to produce substantial torques if required. In order to be able to deliver forces and torques with both signs and with the possibility to produce forces with nominal null torques the number of thrusters is at least 12 but for redundancy in OOS mission is highly recommended to have a full 24 thrusters configuration. Since small thrusters operate mostly without output regulation, a modulation strategy is used to track the desired thrusting action. A classic modulation is PWM but recently interest has shifted

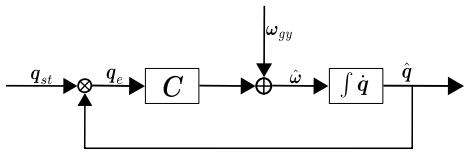

Figure 3: Quaternion complementary filter

to Sigma Delta Modulation (SDM) that has been successfully implemented and ground tested for space applications [51]. It has been shown that comparing with classical PWM the SDM can achieve a lower steady state error and in some cases also leading to lower expenses [21]. After preliminary investigations, it has been decided to use SDM in order to limit fuel usage and achieve better performance.

4.2. Attitude determination & control

There are many sensors and actuators suite that can be derived for attitude control. For the sake of simplicity here will be considered the simplest configuration able to retain significant robustness. The attitude shall be determined using gyroscopes and star trackers while the actuation can be exerted using reaction wheels or thrusters. The estimation paradigm considered is the complementary filter [52] while attitude control laws are determined using an adaptive controller.

4.2.1. Attitude estimation filtering

A complementary filter is a filter that weights in frequency two or more sensors information to refine a state estimate [52]. The simplicity and elegance of the approach can be used also for satellite attitude determination, for example fusing information from a gyroscope and a star tracker. In [52] proof is given for the convergence of the estimate and locally for gyro bias estimation also using quaternions. In Figure 3 a block scheme of this approach for a simple satellite attitude control is presented. Here $\boldsymbol{q}_{st}$ and $\boldsymbol{\omega}_{gy}$ are respectively the measured quaternion from the star tracker and the gyro measured angular velocity. With

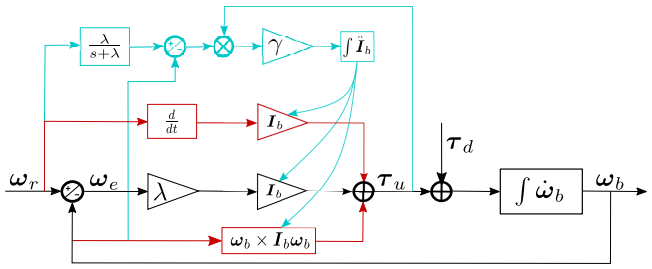

Figure 4: Inertia - adaptive control scheme

$\hat{\boldsymbol{q}}$ and $\hat{\boldsymbol{\omega}}$ are indicated the filter estimated outputs and the quaternion error $\boldsymbol{q}_e$ is computed and fed to the filtering function C with sign consistency.

This filter has some interesting features: it uses a gyro measure to propagate attitude guaranteeing coverage regardless of ambient influence, and it can fuse two sensors measurements at different data rates; can upsample a star tracker with coherence up to gyro datarate; can have good gyro bias rejection; simpler, lighter and easier to tune than a Kalman filter; attitude measurement can be provided by quaternion or vector measurements.

The filter estimated values are used for attitude control, hence an higher sampling rate allows for higher control gain and possibility to track attitude reference with low frequency content. High frequency noise in $\hat{\boldsymbol{q}}$ or $\hat{\boldsymbol{\omega}}$ translates in higher control effort but since the noise induced by sampling difference is limited, it is not going to jeopardize the attitude control robustness.

4.2.2. Attitude control

In order to cope with a non linear time varying system, the attitude control paradigm selected is based on Adaptive Dynamical Inversion. In this controller it is roughly estimated the inertia of the system and the datum is used to generate a control law that follows a specified model.

$$\boldsymbol{\tau_u} = -\text{diag}\left(\hat{\boldsymbol{I}}_b\right) \text{diag}\left(\boldsymbol{\lambda}\right) \left(\boldsymbol{\omega}_b - \boldsymbol{\omega}_{br}\right) + \boldsymbol{\omega}_b \times \left(\text{diag}\left(\hat{\boldsymbol{I}}_b\right) \boldsymbol{\omega}_b\right) + \text{diag}\left(\hat{\boldsymbol{I}}_b\right) \dot{\boldsymbol{\omega}_{br}} \tag{1}$$

Equation (1) shows the centralized adaptive control law where $\boldsymbol{\omega}_b$ is the current measured body angular velocity, $\boldsymbol{\omega}_{br}$ the reference angular velocity for the inner control loop, $\boldsymbol{\lambda}$ the vector of cutoff frequencies per axis and $\hat{\boldsymbol{I}}_b$ the estimated principal inertia components. Second and third components are meant to cancel out the non-linear terms of the dynamical system.

$$\dot{\hat{\boldsymbol{I}}}_b = \gamma \mathrm{diag}\left(\boldsymbol{\omega}_m - \boldsymbol{\omega}_b\right) \boldsymbol{\tau}_{\mathbf{u}} \tag{2}$$

The inertia estimation update is given in Eq. (2) and is meant to estimate the parameter $\hat{\boldsymbol{I}}_b$ such that the controlled system follows the first order reference model. This is a slight modification of the Adaptive Dynamical Inversion control scheme. The canonical implementation, for the system in exam, would see the update equation with terms dependent on the estimated inertia leading to numerical problems [21]. Here the simplified version maintains the characteristics of adaptation while reducing the numerical problems that would otherwise arise.

$$\dot{\boldsymbol{\omega}}_m = \mathrm{diag}\left(\boldsymbol{\lambda}\right)\left(\boldsymbol{\omega}_{br} - \boldsymbol{\omega}_m\right) \tag{3}$$

The simple reference model is presented in Eq. (3) and has $\boldsymbol{\omega}_m \to \boldsymbol{\omega}_{br}$ exponentially. In this model $\boldsymbol{\omega}_m$ is the wanted angular velocity response to the input signal, here taken as a first order lowpass filter. The velocity controller relative to Eq. (1) has the block scheme with adaptive and compensation patterns presented in Figure 4 where $\boldsymbol{\tau}_d$ represent the non-modeled disturbing actions.

$$\boldsymbol{\omega}_{br} = \beta \mathsf{s}\left(\varepsilon\right) \boldsymbol{\eta} + \boldsymbol{\omega}_r \tag{4}$$

The reference angular velocity is given in Eq. (4) where $\boldsymbol{\omega}_r$ is the angular velocity of the tracked attitude reference and $(\boldsymbol{\eta}, \varepsilon)$ the components of the quaternion error computed in the body frame. When $\varepsilon = \pm 1$ and $\boldsymbol{\eta} = 0$ we have null attitude error.

$$\mathsf{s}(\varepsilon) = \begin{cases} +1 & \varepsilon \geq 0 \\ -1 & \varepsilon < 0 \end{cases} \tag{5}$$

To prevent unwinding phenomena, $\mathsf{s}(\varepsilon)$ is used to keep $\boldsymbol{\omega}_{br}(\boldsymbol{\eta}, \varepsilon) = \boldsymbol{\omega}_{br}(-\boldsymbol{\eta}, -\varepsilon)$ and is given as modified sign function in Eq. (5). The velocity reference $\boldsymbol{\omega}_{br}$ is set to achieve quasi-global exponential convergence in the controller outer loop while preventing unwinding.

4.3. Robotic arm guidance & control

The robotic arm is commanded using a decentralized adaptive controller pretty much identical to the attitude control version, except for the non linear compensating terms. Adaptivity plays the same role of the attitude controller since the robot configuration might change or in general some properties of the system might change. For manipulators it is more robust to use a decentralized control since accounting for complex cross coupling effects might reduce the robustness of the whole system, since it is heavily model dependent.

Then, the reference used for such controller needs to account for the whole robot, meaning that the guidance of the robot must be centralized. A simple but not entirely robust possibility is to use the Jacobian of the function that maps the joints position to the end effector pose error with respect to the target. However this approach to determine joint speed that would reduce the error to zero does not account for joint limitations or singularities in the Jacobian. A new approach is here proposed.

4.3.1. Levenberg-Marquardt guidance

A new guidance law has been designed to generate a smooth trajectory that satisfies joints limitations, avoid Jacobian singularities, and has a limited frequency content to ease the controller tracking. The new guidance is composed of two main blocks: one determine the final position the joints have to reach in order to follow the target and the second one translates the final values in a

smooth trajectory that the arm controller can follow. A small addition can be made in order to achieve null error in case of moving target.

First the final state is computed using a non linear minimizer able to work under Jacobian singularities. In formal terms we search for the final joint state $\boldsymbol{\vartheta}_t$ such that the end effector position $\boldsymbol{h}$ is equal to the target location $\boldsymbol{h}_t$ and is also compatible with joints limits. Let us define the pose error $\boldsymbol{e}_{\boldsymbol{h}}(\boldsymbol{\vartheta})$ as the kinematic entity composed by six elements that nullifies when $\boldsymbol{h}(\boldsymbol{\vartheta}) = \boldsymbol{h}_t$ and $\boldsymbol{\vartheta}_t$ the corresponding joint position. In the coding of robotic arm guidance and simulation dual quaternions have been used, but any representation is theoretically viable.

However $\boldsymbol{\vartheta}_t$ must be bounded at least by joint limits as $\boldsymbol{\vartheta}_{min} < \boldsymbol{\vartheta}_t < \boldsymbol{\vartheta}_{max}$. We define a new variable $\boldsymbol{\xi}$ such that

$$\boldsymbol{\vartheta}_t(\boldsymbol{\xi}) = \boldsymbol{\xi} + \frac{\boldsymbol{\vartheta}_{max} + \boldsymbol{\vartheta}_{min}}{2} \tag{6}$$

$$\boldsymbol{\xi}^2 < \left(\frac{\boldsymbol{\vartheta}_{max} - \boldsymbol{\vartheta}_{min}}{2}\right)^2 \tag{7}$$

Let $\boldsymbol{\nu}$ be the dummy variable that would set to zero the error of the following functional

$$\boldsymbol{e}_{\vartheta}(\boldsymbol{\xi}, \boldsymbol{\nu}) = \boldsymbol{\xi}^2 + \boldsymbol{\nu}^2 - \left(\frac{\boldsymbol{\vartheta}_{max} - \boldsymbol{\vartheta}_{min}}{2}\right)^2 \tag{8}$$

We can merge all together into the problem statement. The two variables $\boldsymbol{\xi}$ and $\boldsymbol{\nu}$, each with length equal to the number of joints, can be determined by supplying Eq. (9) to the Levenberg-Marquardt minimizer.

$$(\boldsymbol{\xi},\, \boldsymbol{\nu}) = \arg\min \left(\boldsymbol{e}_{\boldsymbol{h}}(\boldsymbol{\xi})^T \boldsymbol{e}_{\boldsymbol{h}}(\boldsymbol{\xi}) + \boldsymbol{e}_{\vartheta}(\boldsymbol{\xi}, \boldsymbol{\nu})^T \boldsymbol{e}_{\vartheta}(\boldsymbol{\xi}, \boldsymbol{\nu})\right) \tag{9}$$

Then from $(\boldsymbol{\xi},\, \boldsymbol{\nu})$ one can recover the final state $\boldsymbol{\vartheta}_t$ required to drive the end effector towards its target. This procedure enforces the constraint in a robust and stable formulation that has to pay a doubling in number of states supplied to the minimizer. Should be noted that for low relative velocities between the

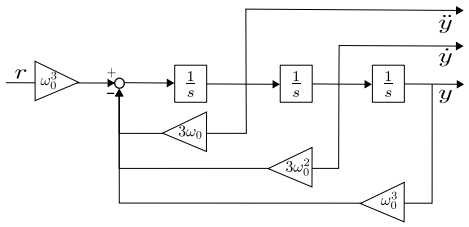

Figure 5: Smoother block scheme

robot and the target, the final state determination can be performed at a lower sample time.

After obtaining compatible $\boldsymbol{\vartheta}_t$, the second step is to feed a proper trajectory to the controller, avoiding to excite the system with step or impulses. Take a lowpass filter of the third order $G(s) = \frac{\omega_0^3}{(s+\omega_0)^3}$ whose block scheme can be found in 5. From any step input given by the minimizer, the filter allows to generate a signal with frequency content lower than the cutoff frequency ω_0 without overshooting.The filter $G(s)$ is thus used as a smoother. Moreover, if we modify the three integrators it is possible to generate a trajectory that accounts also for velocity and acceleration limits coherently. In case of a wide maneuver the second integrator might saturate generating a position signal still within bounds but with limited rate. The acceleration would then modify as well to account for that saturation as the trajectory is feed back to the acceleration level according to the filter weights. Should be noted that saturation at any level will modify the frequency spectrum of the guidance inducing some medium frequency content, still under ω_0.

5. Simulations

The main scenario to test the GNCR closed loop performance sees proximity operations performed by a servicer robot to a customer satellite in LEO. The satellite needs to autonomously hoover at few meter distance from the target, maintain relative attitude and operate the robotic arm to reach a docking port. The whole procedure is summarized in Figure 6.

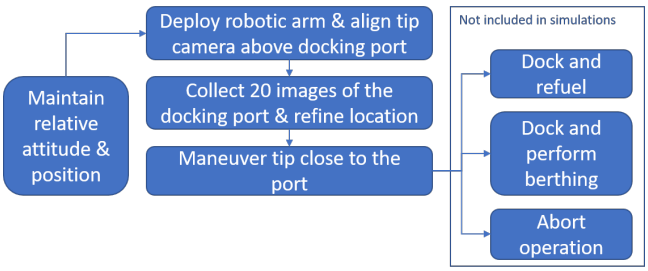

Figure 6: Simulated operations scheme

The first task sees the arm approach the target port at a hovering distance of 20 cm. The position of the port with respect to the target is known with an error of 2, 3 and 1 cm for x, y and z axis respectively. Once this stage is reached, the second phase starts and the camera on the robotic arm takes 21 pictures of the port and an estimation of the real location is made. Then phase three sees the final approach until the port is reached. A final phase has been added to verify the capability of keeping the arm in position. The threshold for reaching the latter stage is mainly related to the estimated distance from the target and is set to 0.5 centimeters.

The effective error in positioning of the end effector depends mainly on the S/C ability to keep a fixed distance with relative estimation errors lower than 5 millimeters and below 0.5 degrees. For some applications the requirements could be even stricter and require a more elaborate estimation scheme, but the goal set is meant to be representative for the early design phases of a GNCR subsystem for OOS. The simulations are carried out using Simulink environment and the robot physical and control data are shown in Table 2.

Figures 7 and 8 present the error in position and attitude of the vision system estimate of the relative state of the customer satellite. In Figure 7 we can appreciate the zero mean quasi-gaussian error of the angles around 3 axis: using small angle assumption the quaternion error elements gives approximately the small angle errors per each axis. In figure 8 we have a similar profile that can be fitted to a Weibull distribution as the quantity depicted is the norm of the

	units	1	2	3	4	5	6	7
				Hardware data				
Link mass	$[kg]$	2.12	42.4	4.24	16.96	2.12	2.12	1.06
Link length	$[m]$	0.10	2.00	0.20	0.80	0.10	0.10	0.05
Link max inertia	$\left[kg \cdot m^2\right]$	0.003	14.16	0.017	0.915	0.003	0.003	0.001
Link min inertia	$\left[kg \cdot m^2\right]$	0.003	0.053	0.0053	0.0212	0.003	0.003	0.001
Max joint position	$[deg]$	180	90	180	0	90	180	180
Min joint position	$[deg]$	-180	-90	0	-180	-90	0	-180
Max joint velocity	$[deg/s]$	1.2	1.2	1.2	1.2	1.2	1.2	1.2
				Controller data				
Reference inertia	$\left[kg \cdot m^2\right]$	7.5	3	1.5	3	1.5	0.15	0.6
Maximum inertia	$\left[kg \cdot m^2\right]$	300	300	30	300	3	0.3	0.3
Minimum inertia	$\left[kg \cdot m^2\right]$	10^{-3}	10^{-3}	10^{-3}	10^{-3}	10^{-3}	10^{-3}	10^{-3}
Reference cutoff frequency	$[Hz]$	0.1	0.1	0.1	0.1	0.1	0.1	0.1
Velocity cutoff frequency	$[Hz]$	0.7	0.6	0.5	0.4	0.3	0.2	0.1
Torque saturation	$[N \cdot m]$	1	1	1	1	1	1	1

Table 2: Robotic arm parameters

error position vector. Looking at the error variation in time, it is possible to roughly appreciate a non-white frequency content that is the result of complex non linear coupling of many aspects like control, vision estimation and dynamical couplings. For reference, the simulated cameras of this simulation have 60 degrees of field of view, unitary focus and generate 1024×1024 pixels gray-scale images at 1 Hz.

Looking at the numerical values of Figures 7 and 8 it can be seen that the estimation error is rather optimistic for a real navigation camera, albeit the low errors can also be due to the simple geometrical model adopted in the image generation, and to the constrained domain for line search. The simulated images do not include blur, dust, or radiation effects on the sensor as well as a simplified Earth model in the background. This might influence any computer vision program lowering performance or robustness. More realistic errors would have approximately twice standard deviation and mean values.

Regardless, we can infer information about the control position error that uses measurements from the estimated position in Figure 9. The error is kept approximately under one centimeter and part of this error is also due to the very low datarate of the vision sensor. Even if a non-delayed upsampling is performed, the frequency content lost by the sampling cannot be retrieved, hence

the error in position control. Increasing the datarate of the vision estimation would reduce the entity of the position error.

Figure 10 shows the errors of measures and estimation of the complementary filter applied to the servicer self attitude estimation, used for regular operations. In the early phases the estimator is compensating for gyroscope bias and thus the estimated error in attitude is larger than the star tracker. When the integral term of the filter sets to the gyro bias and low frequency drift, the estimation quality increases beyond the pure star tracker output. Should be noted that, thanks to the filter nature, the output of the estimator is able to reach 100 Hz, allowing for fine attitude control. Unfortunately this technique cannot be used for position control, as in this case the vision system output is a reference for the controller and not the measurement.

Thanks to good and high frequency estimate the attitude control is able to assure good performance, as testified by the errors depicted in figure 11. Part of this relevant good behavior is that the robotic arm is controlled to follow a trajectory with low frequency content thanks to the guidance law here proposed. Also, the robot guidance is able to guide the end effector towards the docking port; we can appreciate the reduction of the error in figure 12 through the different phases of the maneuver. The error in the terminal phases is highlighted and we can appreciate an error below one centimeter and one degree in attitude. This is based on true values and thus the results show that even with the errors in target estimation of figs. 7 and 8, plus the error in port location compensated during the second phase, plus the error in relative pose control of the base, the robot controller is able to achieve great precision.

With a little safety factor we can use such results to derive requirements for a small docking port for on orbit servicing applications.

Conclusions

On Orbit Servicing close proximity missions require dedicated GNC and robotics, often using vision sensors. In this article a GNC architecture exploit-

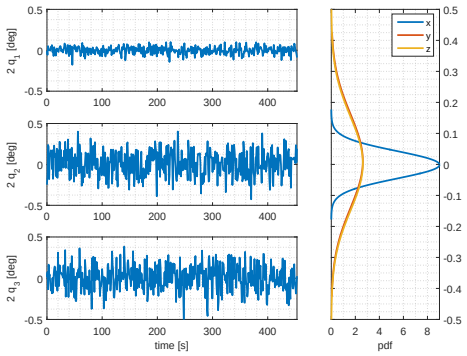

Figure 7: Relative attitude estimation error

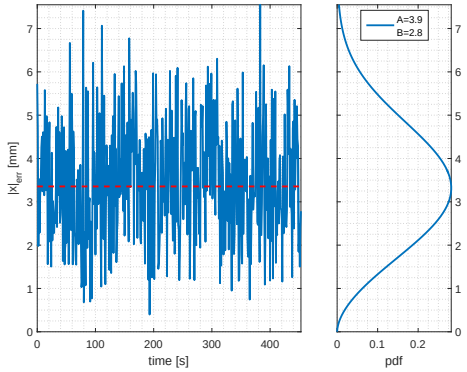

Figure 8: Relative position estimation error

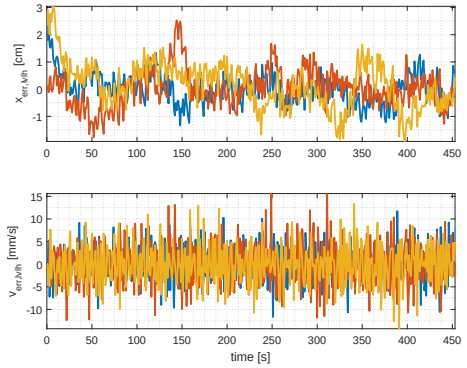

Figure 9: Position control error

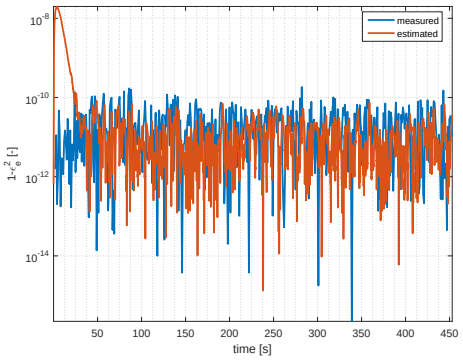

Figure 10: Servicer attitude estimation error

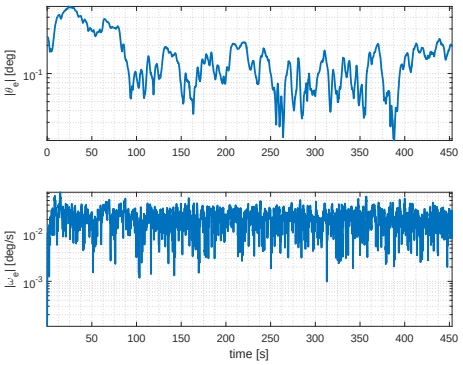

Figure 11: Attitude control errors

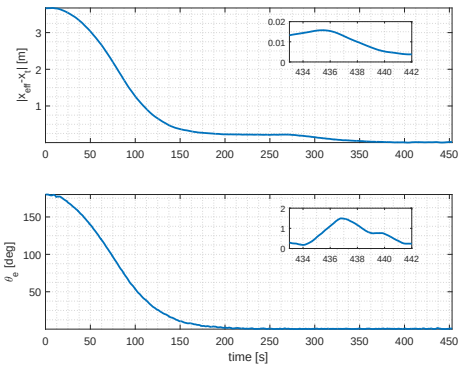

Figure 12: End effector position and attitude distance from the port

ing vision sensors, adaptive control and compliant robotics guidance. To validate the set of control, estimation and robotics algorithms it has been performed a simulation considering also noises, photorealistic images and computer vision elements relevant to the application. Influence among loops (ex: attitude and robotics, vision system and relative positioning) is allowed to verify the robustness of the proposed system to control a satellite in close proximity operations with a customer spacecraft. The proposed architecture shows promising results although the rendering quality of the artificially generated navigation camera images in terms of noises and distortion still needs improvement to yield results comparable with current state of the art space navigation cameras. The relative pose estimation can reach sub-centimeter level at low datarate, the robotic positioning is able to reach similar level of precision without relying on mounted cameras for the final approach. This performance is reached thanks to computer vision relative state estimation and robotics control capability.

Acknowledgements

This work was financed by Italian Ministry of Teaching, Education and Research through the Aerospace Cluster research program 2012, SAPERE-STRONG.

References

[1] J. H. Saleh, E. Lamassoure, D. E. Hastings, Space systems flexibility provided by on-orbit servicing: Part 1, Journal of Spacecraft and Rockets 39 (4) (2002) 551–560.

[2] E. Lamassoure, J. H. Saleh, D. E. Hastings, Space systems flexibility provided by on-orbit servicing: Part 2, Journal of Spacecraft and Rockets 39 (4) (2002) 561–570.

[3] A. Long, M. Richards, D. E. Hastings, On-orbit servicing: a new value proposition for satellite design and operation, Journal of Spacecraft and Rockets 44 (4) (2007) 964–976.

[4] J. H. Saleh, E. S. Lamassoure, D. E. Hastings, D. J. Newman, Flexibility and the value of on-orbit servicing: New customer-centric perspective, Journal of Spacecraft and Rockets 40 (2) (2003) 279–291.

[5] A. M. Long, et al., Framework for evaluating customer value and the feasibility of servicing architectures for on-orbit satellite servicing, Ph.D. thesis, Massachusetts Institute of Technology (2005).

[6] A. Flores-Abad, O. Ma, K. Pham, S. Ulrich, A review of space robotics technologies for on-orbit servicing, Progress in Aerospace Sciences 68 (2014) 1–26.

[7] D. Cornier, D. Paris, B. Dore, F. Thellier, J. Francart, The automated transfer vehicle ATV mission to the international space station, rendezvous and docking aspects, in: International Space Station Conference, Houston, Texas, 1999.

[8] O. Kawasaki, K. Yamanaka, T. Imada, T. Tanaka, The on-orbit demonstration and operations plan of the H-II transfer vehicle (HTV), in: The 51th Int. Astronautical Congress, Rio de Janeiro, Brazil, 2000.

[9] M. Vozoff, The SpaceX dragon spacecraft - a generic platform for in-space experimentation, in: 59th International Astronautical Congress (IAC 2008), Glasgow United Kingdom, 2008.

[10] P. Miotto, Designing and validating proximity operations rendezvous and approach trajectories for the cygnus mission, in: AIAA Guidance, Navigation, and Control Conference, 2010.

[11] R. M. Pinson, R. T. Howard, A. F. Heaton, Orbital express advanced video guidance sensor: ground testing, flight results and comparisons, in: Proceedings of the AIAA Guidance, Navigation and Control Conference and Exhibit, Vol. 1, 2008, pp. 1–9.

[12] R. T. Howard, A. F. Heaton, R. M. Pinson, C. K. Carrington, Orbital express advanced video guidance sensor, in: Aerospace Conference, IEEE, 2008, pp. 1–10.

[13] A. F. Heaton, R. T. Howard, R. M. Pinson, Orbital express AVGS validation and calibration for automated rendezvous, in: AIAA guidance, navigation and control conference and exhibit, Honolulu, United States, 2008, pp. 18–21.

[14] N. F. Dipprey, S. Rotenberger, Orbital express propellant resupply servicing, in: Proceedings of the 39th AIAA/ASME/SAE/ASEE Joint Propulsion Conference and Exhibit, 2003, pp. 20–23.

[15] A. Ogilvie, J. Allport, M. Hannah, J. Lymer, Autonomous satellite servicing using the orbital express demonstration manipulator system, in: Proc. of the 9th International Symposium on Artificial Intelligence, Robotics and Automation in Space, 2008, pp. 25–29.

[16] K. Yoshida, Engineering test satellite VII flight experiments for space robot dynamics and control: theories on laboratory test beds ten years ago, now in orbit, The International Journal of Robotics Research 22 (5) (2003) 321–335.

[17] T. Kasai, M. Oda, T. Suzuki, Results of the ETS-7 mission-rendezvous docking and space robotics experiments, in: Artificial Intelligence, Robotics and Automation in Space, Vol. 440, 1999, pp. 299–306.

[18] Y. Ohkami, M. Oda, NASDA's activities in space robotics, in: Artificial Intelligence, Robotics and Automation in Space, Vol. 440, 1999, pp. 11–18.

[19] K. Yoshida, Space robot dynamics and control: To orbit, from orbit, and future, in: Robotics Research, Springer, 2000, pp. 449–456.

[20] D. Reintsema, K. Landzettel, G. Hirzinger, Dlr's advanced telerobotic concepts and experiments for on-orbit servicing, in: Advances in telerobotics, Springer, 2007, pp. 323–345.

[21] A. Rivolta, Guidance navigation control and robotics for on orbit servicing, in: PhD thesis, Politecnico di Milano, Milan, Italy, 2018.

[22] A. Medina, A. Tomassini, M. Suatoni, M. Avilés, N. Solway, I. Coxhill, I. S. Paraskevas, G. Rekleitis, E. Papadopoulos, R. Krenn, et al., Towards a standardized grasping and refuelling on-orbit servicing for geo spacecraft, Acta Astronautica 134 (2017) 1–10.

[23] S. Moynahan, S. Touhy, et al., Development of a modular on-orbit serviceable satellite architecture, in: Digital Avionics Systems, 2001. DASC. 20th Conference, Vol. 2, IEEE, 2001, pp. 8.D.4.1–8.D.4.12.

[24] A. Ellery, J. Kreisel, B. Sommer, The case for robotic on-orbit servicing of spacecraft: spacecraft reliability is a myth, Acta Astronautica 63 (5) (2008) 632–648.

[25] B. R. Sullivan, D. L. Akin, A survey of serviceable spacecraft failures, Databases 1 (2001) 4540.

[26] W. Xu, B. Liang, B. Li, Y. Xu, A universal on-orbit servicing system used in the geostationary orbit, Advances in Space Research 48 (1) (2011) 95–119.

[27] C. J. Dennehy, J. R. Carpenter, A summary of the rendezvous, proximity operations, docking, and undocking (RPODU) lessons learned from the defense advanced research project agency (DARPA) orbital express (OE) demonstration system mission.

[28] M. Bondy, R. Krishnasamy, D. Crymble, P. Jasiobedzki, Space vision marker system (SVMS), in: AIAA SPACE 2007 Conference & Exposition, 2007, p. 6185.

[29] I. Kawano, M. Mokuno, T. Kasai, T. Suzuki, Result of autonomous rendezvous docking experiment of engineering test satellite-vii, Journal of Spacecraft and Rockets 38 (1) (2001) 105–111.

[30] M. Mokuno, I. Kawano, In-orbit demonstration of an optical navigation system for autonomous rendezvous docking, Journal of Spacecraft and Rockets 48 (6) (2011) 1046–1054.

[31] G. Arantes, E. M. Rocco, I. M. da Fonseca, S. Theil, Far and proximity maneuvers of a constellation of service satellites and autonomous pose estimation of customer satellite using machine vision, Acta Astronautica 66 (9) (2010) 1493–1505.

[32] A. Petit, N. Despré, E. Marchand, K. Kanani, F. Chaumette, S. Provost, G. Flandin, 3D model-based tracking for space autonomous rendezvous, in: 8th International ESA Conference on Guidance and Navigation Control Systems, 2011.

[33] A. Yol, E. Marchand, F. Chaumette, K. Kanani, T. Chabot, Vision-based navigation in low Earth orbit, in: International Symposium on Artificial Intelligence, Robotics and Automation in Space, 2016.

[34] P. J. Besl, N. D. McKay, et al., A method for registration of 3-D shapes, IEEE Transactions on pattern analysis and machine intelligence 14 (2) (1992) 239–256.

[35] D. G. Lowe, Distinctive image features from scale-invariant keypoints, International journal of computer vision 60 (2) (2004) 91–110.

[36] H. Bay, T. Tuytelaars, L. Van Gool, Surf: Speeded up robust features, in: Computer Vision–ECCV, Springer, 2006, pp. 404–417.

[37] H. Bay, A. Ess, T. Tuytelaars, L. Van Gool, Speeded-up robust features (SURF), Computer vision and image understanding 110 (3) (2008) 346–359.

[38] E. Rublee, V. Rabaud, K. Konolige, G. Bradski, ORB: An efficient alternative to SIFT or SURF, in: IEEE international conference on Computer Vision (ICCV), 2011, pp. 2564–2571.

[39] X. Gao, B. Liang, W. Xu, Attitude determination of large non-cooperative spacecrafts in final approach, in: 11th International Conference on Control Automation Robotics & Vision, IEEE, 2010, pp. 1571–1576.

[40] X. Du, B. Liang, W. Xu, Y. Qiu, Pose measurement of large non-cooperative satellite based on collaborative cameras, Acta Astronautica 68 (11) (2011) 2047–2065.

[41] W. Xu, Q. Xue, H. Liu, X. Du, B. Liang, A pose measurement method of a non-cooperative GEO spacecraft based on stereo vision, in: 12th International Conference on Control Automation Robotics & Vision, IEEE, 2012, pp. 966–971.

[42] T. Tzschichholz, T. Boge, H. Benninghoff, A flexible image processing framework for vision-based navigation using monocular image sensors, in: 8th International ESA Conference on Guidance and Navigation Control Systems, 2011.

[43] M. Dunstan, K. Hornbostel, Image processing chip for relative navigation for lunar landing, in: 9th International ESA Conference on Guidance, Navigation, and Control Systems, Porto, Portugal, 2014.

[44] G. Capuano, M. Severi, E. Della Sala, R. Ascolese, C. Facchinetti, F. Longo, Compact and high-performance equipment for vision-based navigation, in: 63rd International Astronautical Congress (IAC), Napoli, Italy, 2012.

[45] G. Capuano, R. Ascolese, D. Titomanlio, P. Longobardi, M. De Nino, G. Formicola, A multi-ocular smart system for vision-based space navigation, in: 65rd International Astronautical Congress (IAC), Toronto, Canada, 2014.

[46] H. Liu, Z. Wang, B. Wang, Z. Li, Pose determination of non-cooperative spacecraft based on multi-feature information fusion, in: IEEE International Conference on Robotics and Biomimetics, 2013, pp. 1538–1543.

[47] M. W. Walker, L. Shao, R. A. Volz, Estimating 3-D location parameters using dual number quaternions, CVGIP: image understanding 54 (3) (1991) 358–367.

[48] B. K. Horn, Closed-form solution of absolute orientation using unit quaternions, JOSA A 4 (4) (1987) 629–642.

[49] M. McCrum, M. Dunstan, S. Parkes, Realistic image generation for testing vision-based autonomous rendezvous, in: 7th International ESA Conference on Guidance, Navigation and Control Systems, 2008.

[50] P. Lunghi, M. Ciarambino, M. Lavagna, A multilayer perceptron hazard detector for vision-based autonomous planetary landing, Advances in Space Research 58 (1) (2016) 131–144. doi:10.1016/j.asr.2016.04.012.

[51] R. Zappulla, J. Virgili-Llop, M. Romano, Spacecraft thruster control via sigma–delta modulation, Journal of Guidance, Control, and Dynamics (2017) 1–6.

[52] R. Mahony, T. Hamel, J.-M. Pflimlin, Nonlinear complementary filters on the special orthogonal group, IEEE Transactions on automatic control 53 (5) (2008) 1203–1218.